AUTOMATED TISSUE CLASSIFICATION IN MRI BRAIN IMAGES WITH THE USE OF DEFORMABLE REGISTRATION

Daniel Schwarz and Tomas Kasparek

Institute of Biostatistics and Analyses, Masaryk University
Kamenice 3, 625 00, Brno, Czech Republic
phone: + (420) 549492854, fax: + (420) 549492855, email: schwarz@iba.muni.cz
web: www.iba.muni.cz

ABSTRACT

Methods of tissue classification in MRI brain images play a significant role in computational neuroanatomy, particularly in automated ROI-based volumetry. A well-known and very simple k-NN classifier is used here without the need for user input during the learning process. The classifier is trained with the use of tissue probabilistic maps which are available in selected digital atlases of brain. The influence of misalignement between images and the tissue probabilistic maps on the classifier's efficiency is studied in this paper. Deformable registration is used here to align the images and maps. The classifier's efficiency is tested in an experiment with data obtained from standard Simulated Brain Database.

1. INTRODUCTION

Methods of brain tissue classification in MRI data are often used in whole-brain morphometry methods, such as voxel-based morphometry [1]. The brain tissues are segmented and their density loss is analysed in voxel-by-voxel tests [2], [3] in order to clarify how the morphological changes implicate neuropsychiatric diseases and to illustrate the relationship between the brain morphology and its function. Despite the vast rate of VBM utilization in the neuroimaging community [4], the conventional region of interest (ROI)-based methods play still an important role and stand for the gold standard in volumetry of anatomical structures. These methods require often manual segmentation, which makes them time-consuming, subjective and error-prone. To address the problem of manual segmentation, a number of automated unbiased techniques emerged. In [5], a deformable registration is used to warp a prelabeled image, which serves as an atlas, to a subject image. Automated segmentation of gross anatomical structures is thus achieved and it is further improved by tissue classification and several heuristic rules.

Methods of image registration are still in the scope of many researchers [6], [7]. The most challenging tasks are connected to intersubject multimodal registration which does not assume that MRI tissue intensities and contrasts remain unchanged across subjects [8], [9]. Even if a high-dimensional registration is used, it cannot be assumed that applying resulting deformations on a prelabeled atlas, a perfect segmentation can be obtained, mainly in small structures with a complex shape, e.g. hippocampus. After deforming a hippocampus mask obtained from an atlas, the voxels belonging into white matter or cerebrospinal fluid classes may be subtracted from the neighbourhood of the mask refining its shape in this way.

In this paper, an algorithm for tissue classification is tested for its further use in atlas-based segmentation. Tissue probability maps are used to train the classifier and the influence of misalignment between images and tissue probabilistic maps on the classifier's efficiency is studied. The misalignment is caused by intersubject anatomical variability and is partially suppressed with the use of deformable registration.

2. METHODS

Efficiency of algorithms for brain tissue segmentation in MRI images is tested here. A simple algorithm, usually used for supervised classification, is tested together with an automated training process based on tissue probabilistic maps. Next, prelabeled image is deformed according to transformation found in deformable registration of an atlas with a target image. Simulated images with ground-truth segmentations are used for evaluation purposes.

2.1 Unsupervised classification

The k-Nearest Neighbour (k-NN) classification rule is proposed here as it is a straightforward and intuitive method. It is a technique for nonparametric supervised pattern classification. It uses a training set of N prototype feature vectors and the corresponding correct classification of each prototype into one of C classes. For a given vector, it searches for the k nearest vectors in the training set according to a given metric, traditionally the Euclidean distance. The class of the vector is then decided by the majority class among the k nearest neighbours [7]. The size of the feature vectors depends on the data to be classified. In the case of MRI brain images the feature vectors contain one or more intensities from T1-weighted, T2-weighted or proton density (PD)-weighted images.

In order to avoid user's input in the training set construction, an automated selection of the prototypes is proposed here. Decisions about the spatial locations of the prototypes are not made by a user but it is done according to tissue probability maps (TPMs). For each spatial location in the stereotaxic space, the TPM value expresses the probability of the occurrence of the given tissue in that location. The spatial prob-

ability distribution represents certain subject population which the particular atlas is made from. In the proposed algorithm, the set of prototypes contains intensities sampled at the most probable locations of main brain tissues occurrences. The same number of prototypes is taken for each of the tissues: white matter (WM), gray matter (GM) and cerebrospinal fluid (CSF) here.

2.2 Deformable registratiom

The algorithm used here for nonlinear multimodal intersubject registration is inspired by Rogelj's approach in [8]. The scheme of the algorithm is in Fig. 1. At first, local translations **f** (usually referred as forces) are calculated at each voxel or pixel as the derivative of a similarity measure. Then, a spatial deformation model is used to compute the displacement **u** of the floating image *N* from the local forces. The process is iterated until a global similarity measure stops increasing. A multiresolution strategy propagating solutions from coarser to finer levels is applied to speed up the convergence of the algorithm and to avoid local optima.
The combined elastic-incremental spatial deformation model proposed in [8] is used here. It combines the elastic and the incremental elastic approach to deformable registration based on continuum mechanics. Its design follows the concept of solving partial differential equation associated with linearized elasticity or viscosity by convolution filtering, where the filter kernel equals the impulse response of the deformable media. The displacement is computed as a reaction of local forces exerted in the floating image *N* by [8]:

$$\begin{aligned} \mathbf{u}_f &= c \cdot \mathbf{f}, \\ \mathbf{u}^{(i)} &= \left(\mathbf{u}^{(i-1)} + \mathbf{u}_f^{(i)} * \mathbf{G}_I\right) * \mathbf{G}_E. \end{aligned} \tag{1}$$

The first part of (11) follows Hook's law to compute unregularized displacements. It says that the points move proportionally to the applied forces **f** with a constant c. The second part of (1) regularizes the displacements by convolution filters $\mathbf{G}_I$ and $\mathbf{G}_E$ which define spatial deformation properties of the modelled material. Gaussian kernel as a separable approximation to the elastic kernel is used here. It does not provide control over compressibility, due to independence of spatial dimensions. While this property is disadvantageous in particular registration tasks, it is required in the case of intersubject registration.

2.3 Synthetic images and deformations

In real biomedical problems, the correct deformations between images or between an image and an atlas are unknown. To assess the quality of automated classification, correctly registered images together with their segmentations in advance are required. Realistic T1 , T2- and proton density (PD)-weighted data with 3% noise and 20% intensity nonuniformity (INU) from the Simulated Brain Database (SBD) are used here for evaluation purposes. The values of noise and INU are reported as typical artifact severity in [10]. Images with voxels classified according to the tissue they represent are available.

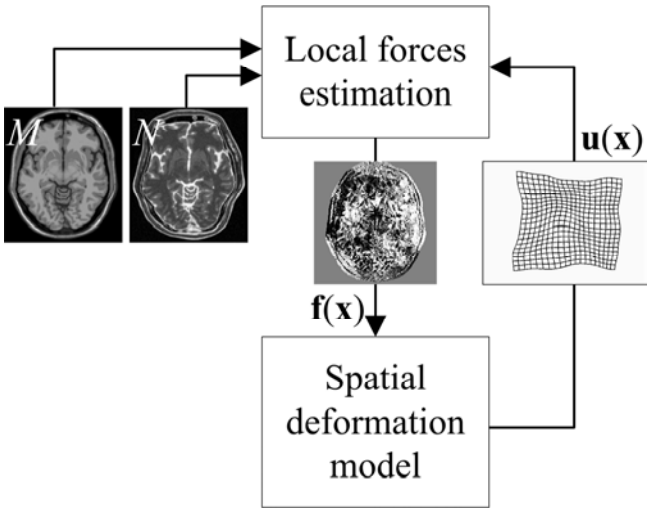

Figure 1 – The scheme of the deformable registration algorithm. The displacement field **u** which maximizes global mutual information between a reference image *M* and a floating image *N* is searched in an iterative process which involves computation of local forces **f** in each individual voxel or pixel and their regularization by Rogelj's elastic-incremental spatial deformation model.

The disadvantage of the evaluation technique may reside in the synthetic character of the initial deformations which may be different from the real intersubject anatomical variability. Thus, the synthetic deformations are produced here by two completely different anatomical variability simulators, which are described further. Additionally, the performance of the proposed methods is evaluated in complex studies involving registration and classification experiments on many images deformed by various synthetic deformations. Due to the computational complexity of the classification and registration methods, the evaluation is done on 2D data. Both anatomical variability simulators are used to produce 20 random, image dependent deformations for 20 transversal slices extracted from T1- and T2-weighted SBD volumes. The deformations are normalized, in order to use them for simulating various degrees of anatomical differences, expressed by the maximum absolute initial displacement $|\mathbf{u}^{init}{}_{MAX}| \in \{5\text{ mm}, 10\text{ mm}, 12\text{ mm}\}$. The maximum value 12 mm was selected according to results of an experiment in which the anatomical variability among 48 real 3D brain images transformed to the stereotaxic space was studied with the use of the deformable registration method described above.

2.3.1 RGsim - simulator based on Rogelj's Gaussians

Rogelj's combined elastic-incremental spatial deformation model is used to regularize random force fields in an iterative process. The standard deviations of the Gaussian convolution filters are set randomly to σ_{GI}=4±2 mm and σ_{GE}=8±2 mm in each iteration. Random forces are generated at 10% randomly selected points from the points which form edges in the image. The maximum force magnitude is gradually decreasing $|\mathbf{f}_{MAX}| \sim K_i/i$, where K_i=3±2 is a randomly preset total number of iterations and i is the current iteration. The diffeomorphicity of the obtained deformation

with $|\mathbf{u}^{init}{}_{MAX}|$=12 mm is checked with the minimum determinant of its Jacobian in each iteration and σ_{GI} and σ_{GE} are linearly increased, if the condition of topology preservation is not met.

2.3.2 TPSsim - simulator based on thin-plate splines

Multilevel deformations with thin-plate splines as basis functions are generated. Forces (translations of control points) are set in centers of blocks. The number of blocks is increasing in the subdivision scheme from 16 in the second level to 4096 in the sixth level (the first level is left out). The translations are set equally to the displacements obtained in previous levels. Only in randomly selected blocks, the translations are set differently to refine the deformation. The probability of the block selection is decreasing P=$0.6^{level-2}$ as well as the maximum force magnitude $|\mathbf{f}_{MAX}|$~$0.75^{level-2}$. The total number of changing translations is 95 on the average. The diffeomorphicity of the obtained deformation with $|\mathbf{u}^{init}{}_{MAX}|$=12 mm is checked with the minimum determinant of its Jacobian in each iteration and P and $|\mathbf{f}_{MAX}|$ are linearly decreased, if the condition of topology preservation is not met.

3. EXPERIMENT AND RESULTS

The experiment included three parts: 1) brain tissue segmentation based on deforming a prelabeled image, 2) k-NN classification with the use of TPMs and 3) k-NN classification with the use of TPMs matched to the classified image with the use of registration results. Each part of the experiment was computed on 20 various 2D images obtained by applying various deformations computed with the simulators described above. The deformations were applied on 20 transversal slices of prelabeled 3D image from SBD and on 20 corresponding slices of T1-weighted image with no added noise or INU artifact. In this way, 20 various templates with ground-truth segmentations were prepared. The images for classification were obtained as the corresponding slices of T2-weighted image with added noise and INU artifact. The average overlap of the labels in T2-weighted images and T1-weighted templates is expressed by the values of J_{init} in tab. 1.

The efficiency of classification J_x in all parts of the experiment was computed for each image as the ratio between the number of correctly labeled pixels and the number of all pixels belonging to GM, WM and CSF classes. Tab. 1 shows the average efficiency computed from 20 classifications.

Deformations of prelabeled images were computed during registrations of T1-weighted templates to T2-weighted images. The elastic-incremental model was set as follows: σ_{GI}=3.5 mm and σ_{GE}=1.5 mm. The average overlaps are expressed as J_{reg} in tab. 1. If the registration was perfect, no drop in overlap would be presented.

The k-NN classifier was trained on 300 prototypes, 100 prototypes for each class, and it sought for the majority class among k=5 nearest neighbours. The onedimensional feature space contained T2-weighted intensities for three various brain tissues. The prototypes were obtained with the use of TPMs which were used in their original form, with the results expressed by J_{kNN} in the tab. 1, as well as in the form of maps geometrically matched to the T2-weighted image with the use of the deformations obtained from the foregoing registrations, with the results expressed by $J_{kNN\text{-}reg}$ in the tab. 1.

Selected segmented and classified images are shown in the fig. 2.

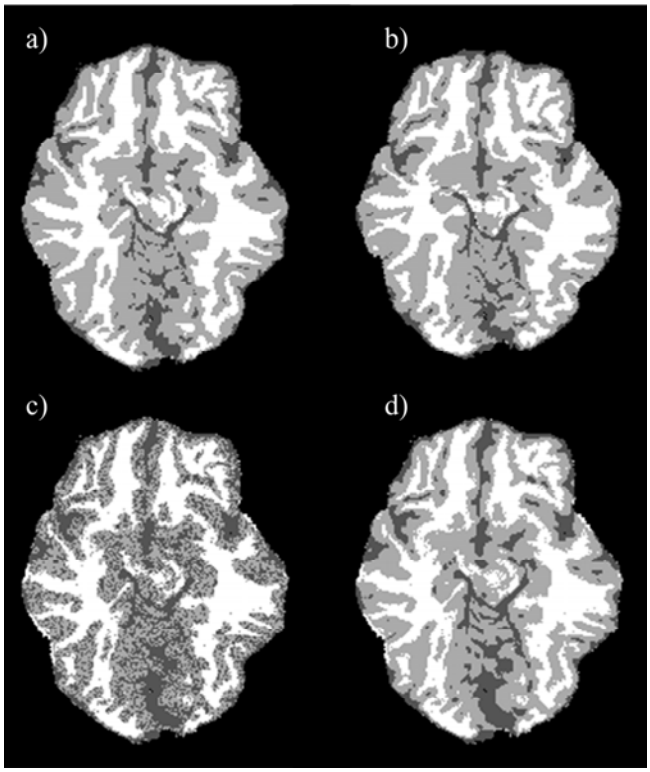

Figure 2 – Selected images with their pixels classified into three classes: gray matter, white matter and cerebrospinal fluid. a) Original SBD labels after deformation, b) labels assigned with the use of deformable registration, c) labels assigned by the k-NN classifier trained with the use of TPMs, d) labels assigned by the k-NN classifier trained with the use of registered TPMs.

Table 1 – Initial average overlaps of the labels in T2-weighted images and T1-weighted templates J_{init} and the classification efficiencies. J_{reg}: labels assigned with the use of deformable registration, J_{kNN}: labels assigned by the k-NN classifier trained with the use of TPMs, $J_{kNN\text{-}reg}$: labels assigned by the k-NN classifier trained with the use of registered TPMs.

$\lvert\mathbf{u}^{\text{init}}{}_{MAX}\rvert$	J_{init} [%]	J_{reg} [%]	J_{kNN} [%]	$J_{kNN\text{-}reg}$ [%]
RGsim				
5 mm	64.3	87.8	79.1	80.0
10 mm	49.8	83.1	74.8	80.3
12 mm	46.3	80.3	73.5	79.8
TPSsim				
5 mm	57.1	89.1	78.2	82.0
10 mm	43.1	86.9	72.2	81.6
12 mm	40.5	84.8	68.3	81.3

4. CONCLUSION

Methods of tissue type classification may play an important role in ROI-based volumetry, as they may be applied in the pipeline of atlas-based segmentation. The classifier may refine shapes of selected anatomical structures found previously by deforming a prelabeled atlas by means of registration. Efficiency of brain tissue classification with the use of simple k-NN method, improved by unsupervised training, was tested here.

It was shown that despite using high-dimensional deformable registration method for atlas-based segmentation, the overlaps of ground-truth segmentations and the segmentations obtained by deforming a prelabeled atlas are not perfect. Additional information from intensity-based classification may therefore help to improve the results. The simple k-NN classifier was tested here, as it is suitable for monomodal as well as multimodal image data. Image data from Simulated Brain Database were used here. A set of prototypes was collected with the use of available tissue probability maps and without user's intervention. The approach to automated training of a classifier presented here is similar to [11]. The main difference lies in the strategy of pruning the set of prototype samples. While the training set is pruned after its acquisition in [11], here the prior information used for training set acquisition is modified before the training phase.

The results showed a considerable influence of the matching between the maps and the classified image on the classifier's efficiency. This fact encourages applying a deformable registration for reducing the intersubject anatomical variability before intensity-based classification rather than using a registration with the use of affine transforms.

REFERENCES

[1] J. Ashburner and K. J. Friston, "Voxel-based morphometry–the methods," *NeuroImage*, vol. 11, pp. 805–821, 2000.

[2] T. Kasparek, R. Prikryl, M. Mikl, D. Schwarz, E. Seskova, and P. Krupa, "Prefrontal but not temporal gray matter changes in males with first-episode schizophrenia," *Progress in Neuro-Psychopharmacology and Biological Psychiatry*, vol. 31, pp. 151–157, 2007.

[3] T. Sigmundsson et al., "Structural abnormalities in frontal, temporal and limbic regions and interconnecting white matter tracts in schizophrenic patients with prominent negative symptoms," *American Journal of Psychiatry*, vol. 158, pp. 234–243, 2001.

[4] K. J. Friston and J. Ashburner, "Generative and recognition models for neuroanatomy," *NeuroImage*, vol. 23, pp. 21–24, 2004.

[5] D. L. Collins, C. J. Holmes, T. M. Peters, and A. C. Evans, "Automatic 3D model-based neuro-anatomical segmentation," *Human Brain Mapping*, vol. 3, pp. 190–208, 1995.

[6] B. Zitova and J. Flusser, "Image registration methods: a survey," *Image and Vision Computing*, vol. 21, pp. 977–1000, 2003.

[7] J. S. Suri, D. L. Wilson, and S. Laxminarayan, *Handbook of Biomedical Image Analysis: Registration Models*. New York: Kluwer Academic Plenum Publishers, 2005.

[8] P. Rogelj, S. Kovacic and J. C. Gee, "Point similarity measures for non-rigid registration of multi-modal data," *Computer Vision and Image Understanding*, vol. 92, pp. 112–140, 2003.

[9] E. D'Agostino, F. Maes, D. Vandermuelen and P. Suetens, "A viscous fluid model for multimodal non-rigid image registration using mutual information," *Medical Image Analysis*, vol. 7, pp. 541–548, 2003.

[10] J. G. Sled, A. P. Zijdenbos and A. C. Evans, "A nonparametric method for automatic correction of intensity nonuniformity in MRI data," *IEEE Transactions on Medical Imaging*, vol. 17, pp. 87–97, 1998.

[11] C. A. Cocosco, A. P. Zijdenbos, and A. C. Evans, "A fully automatic and robust brain MRI tissue classification method," *Medical Image Analysis*, vol. 7, pp. 513–527, 2003.